

## Supplementary Materials for

### The L-type amino acid transporter LAT1 inhibits osteoclastogenesis and maintains bone homeostasis through the mTORC1 pathway

Kakeru Ozaki, Takanori Yamada, Tetsuhiro Horie, Atsushi Ishizaki, Manami Hiraiwa, Takashi Iezaki, Gyujin Park, Kazuya Fukasawa, Hikari Kamada, Kazuya Tokumura, Mei Motono, Katsuyuki Kaneda, Kazuma Ogawa, Hiroki Ochi, Shingo Sato, Yasuhiro Kobayashi, Yun-Bo Shi, Peter M. Taylor, Eiichi Hinoi\*

\*Corresponding author. Email: hinoi@p.kanazawa-u.ac.jp

Published 9 July 2019, *Sci. Signal.* **12**, eaaw3921 (2019)  
DOI: 10.1126/scisignal.aaw3921

#### This PDF file includes:

- Fig. S1. Expression of genes encoding amino acid transporters in preosteoclasts and osteoblasts.
- Fig. S2. Expression of *Slc7a5* mRNA in mutant mice.
- Fig. S3. Phosphorylation of p70S6K1 by EAA deprivation in osteoclasts.
- Fig. S4. Effect of RANKL on [<sup>125</sup>I]IMT incorporation in osteoclasts.
- Fig. S5. Phosphorylation of eIF2 $\alpha$  in *Slc7a5*-deficient cells.
- Fig. S6. Effects of Akt and NF- $\kappa$ B inhibitors in *Slc7a5*-deficient cells.
- Table S1. List of primers used for real-time PCR.

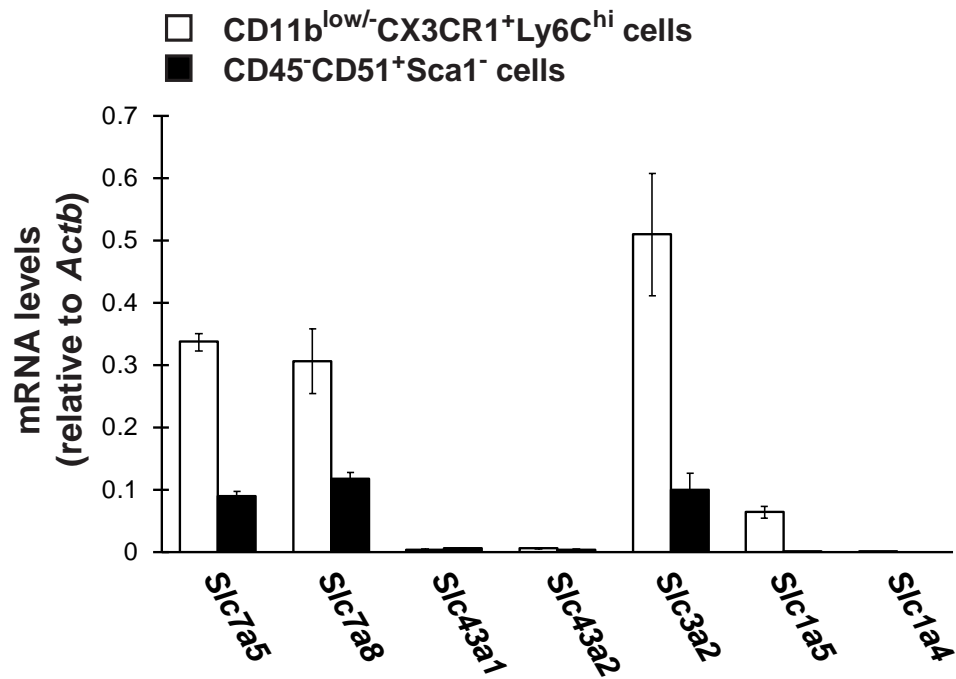


**Fig. S1. Expression of genes encoding amino acid transporters in preosteoclasts and osteoblasts.** CD11b<sup>low/-</sup>-CX3CR1<sup>+</sup>Ly6C<sup>hi</sup> cells (preosteoclasts) and CD45<sup>-</sup>CD51<sup>+</sup>Sca1<sup>-</sup> cells (osteoblasts) were isolated by flow cytometry, and subsequently the expression of transcripts for amino acid transporters were quantified relative to a reference RNA (*Actb*). *n* = 5 mice.

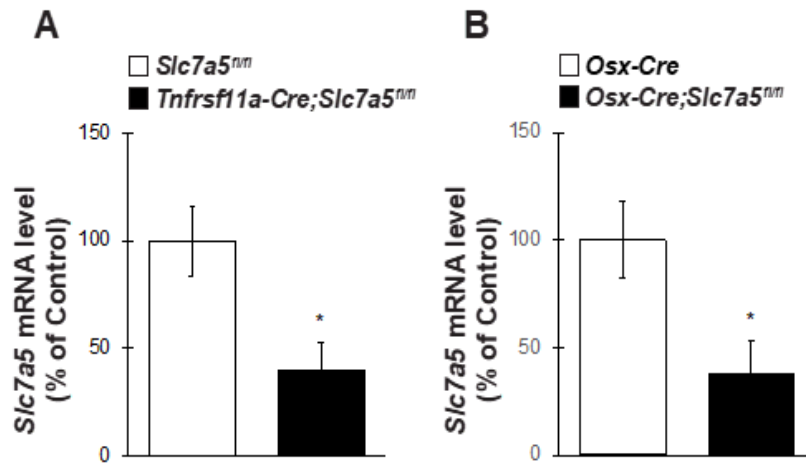


**Fig. S2. Expression of *Slc7a5* mRNA in mutant mice.** Quantitative data for *Slc7a5* expression in (A) Fig. 2B and (B) Fig. 3B.

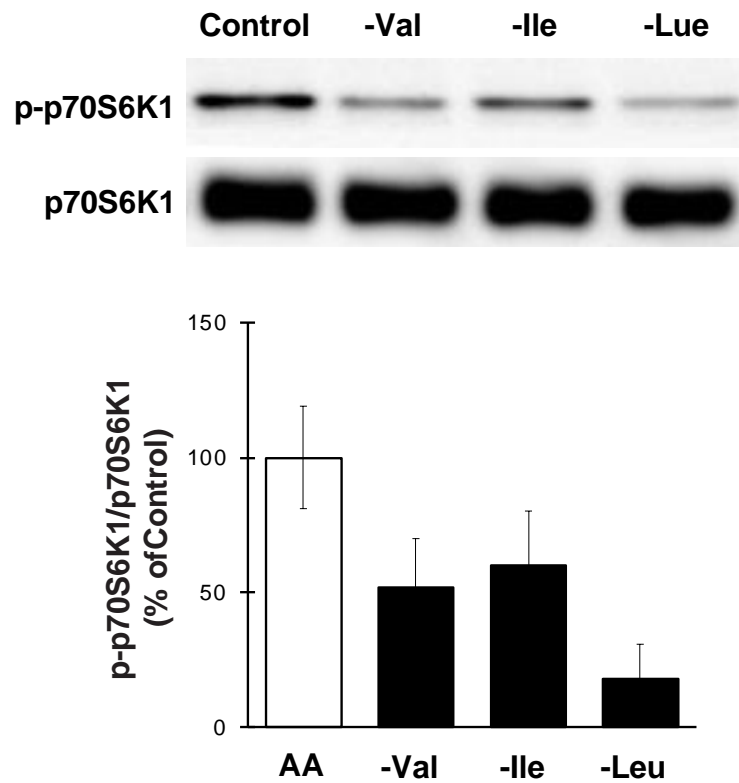


**Fig. S3. Phosphorylation of p70S6K1 by EAA deprivation in osteoclasts.** BMMs derived from *Slc7a5<sup>fl/fl</sup>* mice were retrovirally infected with Cre recombinase and subsequently stimulated with RANKL in the absence of Val, Ile, or Leu, followed by determination of p70S6K1 phosphorylation.  $n = 4$  cell cultures. Data were analyzed by the one-way ANOVA with Bonferroni/Dunnnett post hoc test.

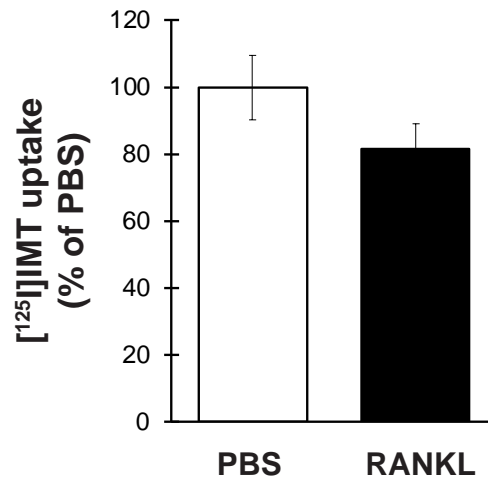


**Fig. S4. Effect of RANKL on [<sup>125</sup>I]JMT incorporation in osteoclasts.** Primary osteoclasts from WT mice were incubated with [<sup>125</sup>I]JMT at 37 °C for 30 min in HBSS buffer in the presence of RANKL. *n* = 4 cell cultures from different mice. Data were analyzed by the two-tailed Students' *t*-test.

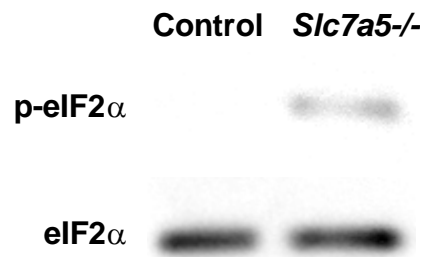


**Fig. S5. Phosphorylation of eIF2 $\alpha$  in *Slc7a5*-deficient cells.** BMMs derived from *Slc7a5*<sup>fl/fl</sup> mice were retrovirally infected with Cre recombinase, followed by determination of eIF2 $\alpha$  phosphorylation.  $n = 4$  mice per genotype.

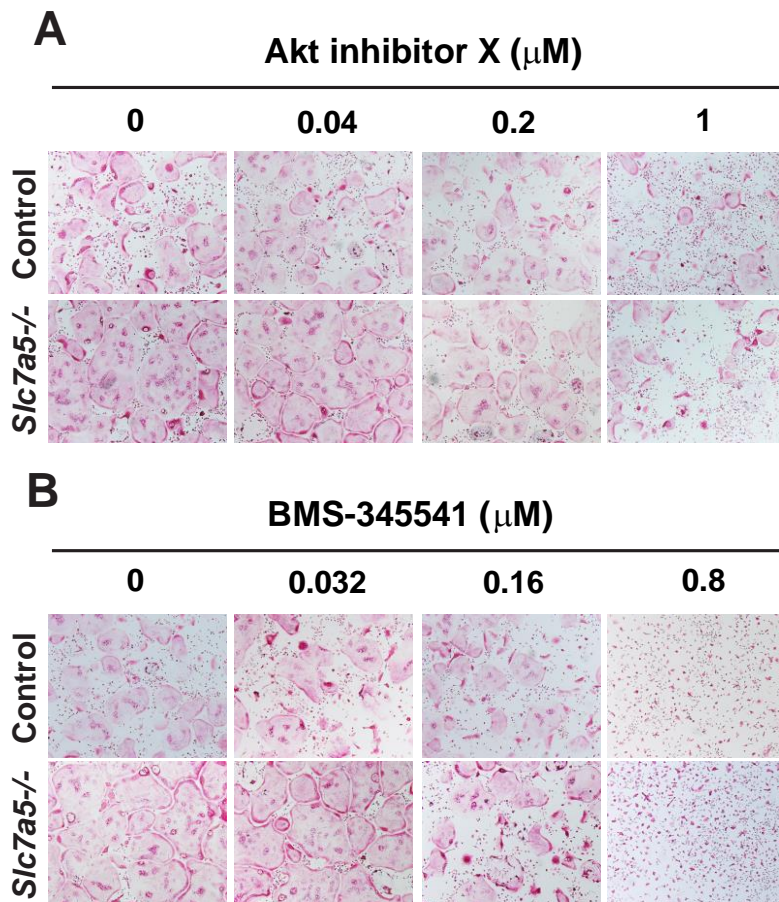


**Fig. S6. Effects of Akt and NF- $\kappa$ B inhibitors in *Slc7a5*-deficient cells.** BMMs from *Slc7a5*<sup>fl/fl</sup> mice were retrovirally infected with Cre recombinase, and subsequently stimulated with different concentrations of (A) Akt inhibitor X or (B) IKK inhibitor (BMS-345541) in the presence of RANKL, followed by TRAP staining.  $n = 4$  mice per genotype.

**Table S1. List of primers used for real-time PCR.**

<b>Genes</b>	<b>Upstream (5'-3')</b>	<b>Downstream (5'-3')</b>
<i>Ctsk</i>	GAAGAAGACTCACCAGAAGCAG	TCCAGGTTATGGGCAGAGATT
<i>Dstamp</i>	GACCTTGGGCACCAGTATTT	CAAAGCAACAGACTCCCAAA
<i>Mmp9</i>	CTGGACAGCCAGACACTAAAG	CTCGCGGCAAGTCTTCAGAG
<i>Nfatc1</i>	CCCGTTGCTTCCAGAAAATA	CCCGTTGCTTCCAGAAAATA
<i>Slc7a5</i>	CTGGTCTTCGCCACCTACTT	GCCTTTACGCTGTAGCAGTTC
<i>Slc7a8</i>	ACGTTTGGTGGAGTCAATGG	CAGGGCTGGGATTGGAGTG
<i>Slc43a1</i>	CTTCCGGGCTTCACCTATCTG	CCCAATTCCAAATCGCATCCAC
<i>Slc43a2</i>	TGCACCGCTGTGTTGGAAA	CCGTGCTGTTAGTGACATTCTC
<i>Slc3a2</i>	CACCGGCTTATCCAAGGAGG	GATGGCTCTTCAGACCAGCTA
<i>Slc1a5</i>	TGGAGGGAATGAACATCCTGG	GTTGAAGAAACGAATGAGCAGC
<i>Slc1a4</i>	GGCATCGCTGTTGCTTACTTC	CGAGGAAAGAGTCCACTGTCT